Broad 4-Hydroxyphenylpyruvate Dioxygenase Inhibitor Herbicide Tolerance in Soybean with an Optimized Enzyme and Expression Cassette[W][OPEN]

Daniel L. Siehl*, Yumin Tao, Henrik Albert, Yuxia Dong, Matthew Heckert, Alfredo Madrigal, Brishette Lincoln-Cabatu, Jian Lu, Tamara Fenwick, Ericka Bermudez, Marian Sandoval, Caroline Horn, Jerry M. Green, Theresa Hale, Peggy Pagano, Jenna Clark, Ingrid A. Udranszky, Nancy Rizzo, Timothy Bourett, Richard J. Howard, David H. Johnson, Mark Vogt, Goke Akinsola, and Linda A. Castle

DuPont Pioneer, Hayward, California 94545 (D.L.S., Y.T., H.A., Y.D., M.H., A.M., B.L.-C., J.L., T.F., E.B., M.S., C.H., I.A.U., L.A.C.); DuPont Stein-Haskell Research Center, Newark, Delaware 19711 (J.M.G., T.H., P.P., J.C.); DuPont Experimental Station, Wilmington, Delaware 19803 (N.R., T.B., R.J.H.); and DuPont Pioneer, Johnston, Iowa 50131 (D.H.J., M.V., G.A.)

With an optimized expression cassette consisting of the soybean (*Glycine max*) native promoter modified for enhanced expression driving a chimeric gene coding for the soybean native amino-terminal 86 amino acids fused to an insensitive shuffled variant of maize (*Zea mays*) 4-hydroxyphenylpyruvate dioxygenase (HPPD), we achieved field tolerance in transgenic soybean plants to the HPPD-inhibiting herbicides mesotrione, isoxaflutole, and tembotrione. Directed evolution of maize HPPD was accomplished by progressively incorporating amino acids from naturally occurring diversity and novel substitutions identified by saturation mutagenesis, combined at random through shuffling. Localization of heterologously expressed HPPD mimicked that of the native enzyme, which was shown to be dually targeted to chloroplasts and the cytosol. Analysis of the native soybean HPPD gene revealed two transcription start sites, leading to transcripts encoding two HPPD polypeptides. The N-terminal region of the longer encoded peptide directs proteins to the chloroplast, while the short form remains in the cytosol. In contrast, maize HPPD was found almost exclusively in chloroplasts. Evolved HPPD enzymes showed insensitivity to five inhibitor herbicides. In 2013 field trials, transgenic soybean events made with optimized promoter and HPPD variant expression cassettes were tested with three herbicides and showed tolerance to four times the labeled rates of mesotrione and isoxaflutole and two times the labeled rates of tembotrione.

For nearly 2 decades, maize (*Zea mays*), soybean (*Glycine max*), and cotton (*Gossypium hirsutum*) farmers have relied on glyphosate and glyphosate-resistant crops for weed control. While favored for its efficacy, economy, and convenience, the onset of glyphosate-resistant weeds, now numbering 29 species (Heap, 2014), signals a need for new herbicide and trait systems as effective as glyphosate (Green and Castle, 2010; Duke, 2012). Unfortunately, prospects for novel herbicide chemistries are not encouraging (Duke, 2012).

Our interest is in the development of crops tolerant to the 4-hydroxyphenylpyruvate dioxygenase (HPPD; EC 1.13.11.27) inhibitors that disrupt pigment production in plants (Fig. 1). Disruption of the conversion of Tyr, through 4-hydroxyphenylpyruvate (HPP), to homogentisate leads to failure to produce plastoquinone essential for photosynthetic electron transfer, leading to the loss of carotenoid pigments and photosynthesis failure (Moran, 2014). Plastoquinone is an essential cofactor for phytoene desaturase in the carotenoid biosynthesis pathway (Ruiz-Sola and Rodriguez-Conception, 2012). Plants lacking carotenoids cannot protect themselves from the radicals generated by the light activation of chlorophyll, causing bleaching, necrosis, and death (Fig. 1C). Further evidence shows that in the absence of carotenoids, the photosynthetic apparatus is not properly assembled (Sozer et al., 2010), explaining why only the new leaves in the plant in Figure 1C are white. Although plastoquinone is also requisite for tocopherol biosynthesis, tocopherol deficiency is not associated with an herbicidal phenotype (Maeda and DellaPenna, 2007). HPPD inhibitors are most effective on broad-leaf weeds but control some grasses as well. Currently, HPPD herbicides are selective for use in maize, while soybeans and other dicot crop species are sensitive.

A broad-spectrum HPPD tolerance trait in soybeans, used in combination with glyphosate tolerance and other traits or selective herbicides, will prolong the positive impact of the glyphosate systems and slow the appearance of resistant weeds. Weed resistance to HPPD-inhibiting herbicides was unknown until two cases involving *Amaranthus* spp. were reported recently (Heap, 2014). Two transgenic soybean crop products, one for tolerance to isoxaflutole (APHIS, 2009) and the other to mesotrione

* Address correspondence to dan.siehl@pioneer.com.

The author responsible for distribution of materials integral to the findings presented in this article in accordance with the policy described in the Instructions for Authors (www.plantphysiol.org) is: Daniel L. Siehl (dan.siehl@pioneer.com).

[W] The online version of this article contains Web-only data.

[OPEN] Articles can be viewed online without a subscription.

www.plantphysiol.org/cgi/doi/10.1104/pp.114.247205

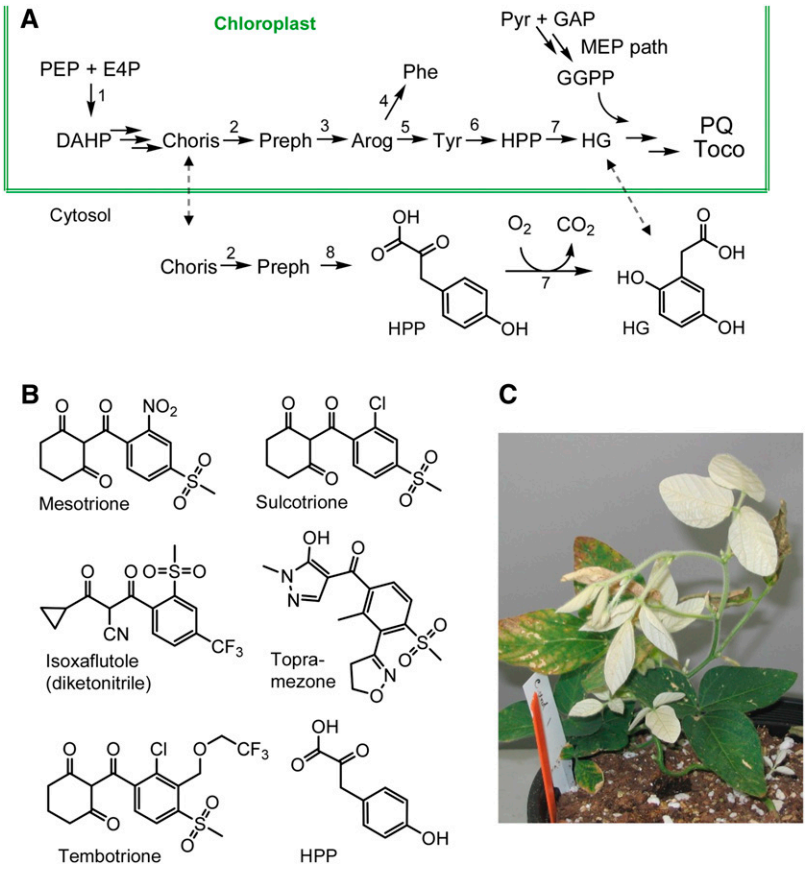

Figure 1. A, HPPD pathway in plants. Prior and present data support an entirely chloroplastic location for HPPD and the aromatic, isoprenoid (2-C-methyl-D-erythritol 4-phosphate [MEP]), plastoquinone (PQ), and tocochromanol (Toco) pathways in monocots, with the exception of reaction 6, for which there are no data in monocots. Legumes have cytosolic chorismate mutase (2), PDH (8), and HPPD (7), hypothetically comprising a cytosolic minipathway wherein PDH bypasses prephenate aminotransferase (3), arogenate dehydrogenase (5), and Tyr aminotransferase (6). Hypothetical metabolite transporters are indicated with dotted arrows. Other reactions shown are 3-deoxy-D-arabinoheptulosonate-7-phosphate synthase (1) and arogenate dehydratase (4). E4P, Erythrose-4-phosphate; GAP, glyceraldehyde-3-phosphate; GGPP, geranylgeranyl diphosphate; HG, homogentisate; PEP, phospho*enol*pyruvate; Pyr, pyruvate. B, Structures of herbicidal HPPD inhibitors and substrate 4-hydroxyphenylpyruvate. C, Bleaching symptoms of HPPD inhibition in soybean caused by mesotrione.

and isoxaflutole (APHIS, 2012), are in the U.S. Department of Agriculture deregulation approval process. The former uses a *Pseudomonas fluorescens* HPPD with a single amino acid change (Matringe et al., 2005), while the latter uses HPPD from oat (*Avena sativa*) with a single amino acid change (Hawkes et al., 2010). Our goal was to develop soybean lines with tolerance to a broad spectrum of HPPD inhibitors.

To develop a robust and stable HPPD tolerance trait in soybean, we sought first to understand the basic biology of the process, including expression of the native gene and localization of native and transgenic proteins, and to evaluate the efficacy of low to moderate expression of a desensitized protein. Data regarding the subcellular location of HPPD are ambiguous, perhaps resulting from species diversity. Early work with organelle fractions attributed most HPPD activity to the chloroplast in spinach (*Spinacia oleracea*; Fiedler et al., 1982) or *Lemna gibba* (Löffelhardt and Kindl, 1979). Organelle targeting can be conjectured from the observation that the N-terminal sequence of mature HPPD isolated from maize leaf begins at either Ala-17 (Fritze et al., 2004) or Ala-23 (Yang et al., 2004) with respect to the translated full-length gene. Two HPPD genes identified from EST libraries prepared from cotton tissue were 98.6% identical, each with a 23-amino acid sequence deemed likely to function in chloroplast targeting by analysis with the ChloroP prediction program (Moshiri et al., 2007). In the same study, tomato (*Solanum lycopersicum*) but not *Brassica* spp. HPPD was predicted to have a chloroplast-targeting peptide (CTP). Subcellular fractionation supported a cytosolic location of the carrot (*Daucus carota*) cell enzyme (Garcia et al., 1997). The same authors determined that after PSORT analysis failed to identify a targeting signal within the Arabidopsis (*Arabidopsis thaliana*) HPPD amino acid sequence, native Arabidopsis HPPD heterologously expressed in tobacco (*Nicotiana benthamiana*) was located exclusively in the cytosol (Garcia et al., 1999). In this study, fluorescent protein markers and microscopy allowed us to clearly visualize the subcellular localization of the native protein or that expressed from HPPD promoters, revealing the localization of HPPD exclusively in the chloroplasts of maize and in both chloroplasts and the cytosol of soybean.

We used bioinformatics analysis of HPPD genomic, EST, and protein sequences to predict active genes and subcellular localization motifs followed by in planta validations. HPPD variants created by directed evolution were screened for insensitivity with multiple HPPD herbicide inhibitors, and transgenic soybean plants expressing the improved HPPD genes were evaluated with multiple herbicides in greenhouse and field trials. Bringing together our understanding of the HPPD genes, proteins, and pathway in soybean, we achieved broad-spectrum HPPD tolerance that will contribute to future best practices (Norsworthy et al., 2012) in integrated weed control.

RESULTS

Bioinformatic and Functional Localization Analyses of Maize HPPD

A single HPPD gene was identified in maize via genomic and EST database searches (National Center for Biotechnology Information [NCBI] reference sequence NM_001112312.1), giving rise to a 444-amino acid encoded protein (Fig. 2A). ProtComp 9.0 (http://linux1.softberry.com/berry.phtml) predicts a cytosolic location of maize HPPD (cytoplasmic score 9.91 out of 10). Similarly, WoLF PSORT (Horton et al., 2007) and TargetP (Emanuelsson et al., 2000) predict a cytosolic location of the HPPD protein. PCLR (Schein et al., 2001) predicts nonchloroplast localization (0.25 with a 0.42 threshold), Protein Prowler (Hawkins and Bodén, 2006) predicts either a mitochondrial (0.34) or chloroplast (0.39) location, and MultiLoc (Höglund et al., 2006) predicts an extracellular (0.74) localization with the first 50 amino acids of maize HPPD but a strong chloroplast localization (0.97) for the full maize HPPD sequence.

Immunolocalization electron microscopy of maize tissue sections was carried out to detect native HPPD localization. Gold labeling was observed mainly in bundle sheath chloroplasts (Supplemental Fig. S1). Particles were also found in mesophyll chloroplasts, but in no other structures. To functionally corroborate the localization of maize HPPD, a binary plant transformation vector was constructed in which the portion of the maize HPPD gene coding for the N-terminal 50 amino acids was fused to the gene coding for *Discosoma* spp. RED FLUORESCENT PROTEIN2 (DsRed2), all under the control of the maize Rubisco activase promoter. A positive control vector was identical except that the DsRed2 insert was fused to the CTP of maize Rubisco activase, while a negative control was DsRed2 with no targeting sequence. The plasmids were transformed into *Agrobacterium tumefaciens* strain AGL-1, and agroinfiltration was used to introduce the constructs into plant cells for transient expression. Leaves of 3-week-old maize seedlings were infiltrated with the *A. tumefaciens* and examined by fluorescence microscopy of hand sections 2 d later. When DsRed2 was fused to Rubisco activase CTP, red fluorescence was seen in discrete packets in a pattern resembling perinuclear chloroplasts, as expected (Fig. 2A). A similar pattern was seen when DsRed2 was fused to the N-terminal 50 amino acids of maize HPPD (Fig. 2B). Without targeting, fluorescence was diffuse, with some concentration in the nucleus (Fig. 2C). In another experiment confirming these results, maize leaf tissue was cobombarded with DNA from both the DsRed2-containing test plasmids and a plasmid encoding untargeted cycle 3 GFP (C3GFP). Transformation of guard cells with vectors encoding either Rubisco activase CTP-DsRed2 or the N-terminal 50 amino acids of maize HPPD fused to DsRed2 clearly resulted in plastid targeting of the DsRed2 reporter, whereas untargeted C3GFP showed no overlap with the DsRed2 signal (Supplemental Fig. S2).

To determine the length of the functional CTP for maize HPPD, vectors were constructed in which the portion of the maize HPPD gene coding for the N-terminal 0, 10, 20, 30, 40, or 50 amino acids was fused to the gene coding for DsRed2 and evaluated with transient expression following the agroinfiltration of maize leaves. Microscopy revealed that 50 amino acids of the maize HPPD N terminus effectively targeted DsRed2 to plastids (Fig. 2F), but 40 amino acids or fewer failed to do so, with DsRed2 fluorescence visible only in the cytoplasm (Fig. 2, D and E). This result indicates that more than 40 amino acids of the N terminus are required for chloroplast localization and that 50 amino acids are sufficient for targeting.

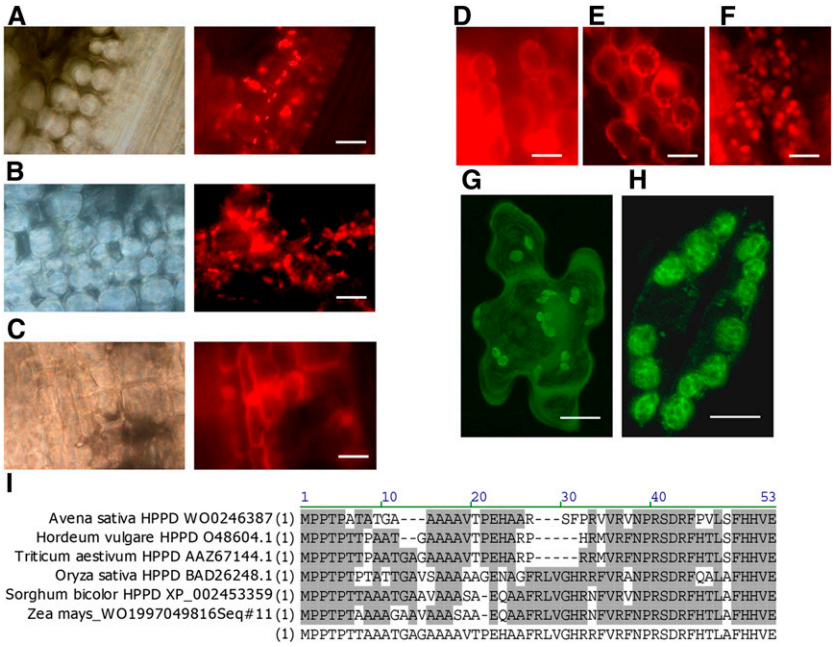

Figure 2. Maize HPPD protein characterization. A, Fluorescence observed in chloroplasts of maize leaf expressing Rubisco activase CTP-DsRed2. B, Fluorescence observed in chloroplasts of maize leaf expressing the N-terminal 50 amino acids of maize HPPD-DsRed2. C, Fluorescence observed in cytosol of maize leaf expressing untargeted DsRed2. Photographs on the left were of the same samples taken with white light. D to F, Maize cells transiently expressing DsRed2 fused to 30-, 40-, and 50-amino acid N-terminal regions of the HPPD protein sequence. G, Expression in both chloroplasts and cytoplasm of soybean leaf epidermal cells transiently expressing AcGFP1 fused to amino acids 1 to 50 of maize HPPD. H, Expression in chloroplasts of guard cells in soybean stably expressing AcGFP1 linked to amino acids 1 to 50 of maize HPPD. I, Alignment of monocot HPPD N-terminal region sequences and consensus monocot functional CTP. Sources of sequences are indicated. Gray shading shows identities in sequences. Bars = 50 μm (A–F), 10 μm (G), and 5 μm (H).

To investigate if the maize HPPD protein is unique, several monocot sequences were compared. The rice (*Oryza sativa*) HPPD N-terminal sequence effectively targeted DsRed2 to maize plastids (data not shown). Furthermore, 50 amino acids of the maize HPPD N terminus delivered DsRed2 to sorghum (*Sorghum bicolor*) chloroplasts. Figure 2I provides an N-terminal alignment of monocot HPPD proteins having identities of 59% to 85%. A consensus monocot HPPD CTP sequence (Fig. 2I) targeted the DsRed2 protein to maize chloroplasts. These data strongly suggest that monocot HPPD proteins share a homologous chloroplast-targeting motif and function.

The function of the monocot HPPD sequence in dicots was explored by transient expression in bush bean (*Phaseolus vulgaris*), tobacco, and soybean cells. The sequence encoding the first 50 amino acids of the maize HPPD protein was fused to a gene encoding *Aequorea coerulescens* GFP1 (AcGFP1) and inserted into a binary expression vector under the control of the Arabidopsis UBIQUITIN10 promoter. A positive control vector was identical except that the AcGFP1 coding region was fused to the 6H1 synthetic CTP (Lassner and Wilkinson, 2008), while a negative control was AcGFP1 with no targeting sequence. The first 50 amino acids of maize HPPD were sufficient to drive the chloroplast import of AcGFP1 in epidermal cells of bush bean, although some green fluorescence remained in the cytoplasm (data not shown). In tobacco, AcGFP1 remained in the cytoplasm, with none apparent in the chloroplasts (data not shown). Results by bombardment in soybean showed AcGFP1 in both plastids and cytoplasm (Fig. 2G). This shows that the maize HPPD CTP is recognized in some dicot plant species but may be inefficiently processed. Stably transformed soybean plants expressing the 50-amino acid N-terminal CTP fused to AcGFP1 showed strong fluorescence in the chloroplasts (Fig. 2H), suggesting that the inefficient translocation observed in transient expression conditions may be due to the high template concentration.

Bioinformatic and Functional Localization Analyses of Soybean HPPD

Soybean is a polyploid derived from two evolutionary genome duplications (Schmutz et al., 2010) and as such appears to have multiple paralog HPPD genes. As some of the annotated genes appear incomplete or have rare ESTs, we focused here on glyma14g03410.1 on chromosome 14. This soybean HPPD protein has been annotated previously as a 449-amino acid protein with N-terminal sequence MPIPMCNEIQ (Cahoon and Coughlan, 2007; sequence 36) and as a 443-amino acid protein with N-terminal sequence MCNEIQAQAQ (GenBank accession no. ABQ96868). Our analysis of genomic and EST data revealed that an in-frame N-terminal extension of the previously annotated coding region exists, adding 41 amino acids to produce a 490-amino acid full-length HPPD protein, as shown in Figure 3A.

5′ RACE revealed two major transcripts for the native soybean HPPD gene. Cloning and sequencing of these PCR products revealed a shorter transcript starting at position +1 able to support translation of the 449-amino acid protein. The longer transcript began at position −237 and comprised the full 490-amino acid open reading frame (ORF; Fig. 3A). Linked in vitro transcription and translation indicated that both mRNAs were translated and made the predicted sized proteins (truncated for convenience in Fig. 3B). The +1 transcript was translated to produce a single protein, designated the short protein. The −237 transcript yielded two proteins, with the lower M_r band at the same molecular weight as the single protein produced from the +1 transcript, suggesting that translation initiated at both positions on the long transcript. The protein produced from the −237 transcript is designated the long protein.

Bioinformatic evaluation of the shorter soybean HPPD sequence did not predict a chloroplast or other targeting sequence. However, a chloroplast-targeting function is predicted for the N-terminally extended form by ProtComp 9.0 (http://linux1.softberry.com), WoLF PSORT (Horton et al., 2007), and PCLR (Schein et al., 2001). TargetP (Emanuelsson et al., 2000) suggests chloroplast localization but gives a higher score to other, while MultiLoc2 (Blum et al., 2009) predicts a cytoplasmic localization for both the first 42 and the first 86 amino acids of the long protein. Functional analysis was required to clarify the predictions.

Transient (Fig. 3C) or stable (Fig. 3, D and E) expression experiments indicated that the long HPPD protein is imported to chloroplasts, while the short protein remains in the cytosol. Plant expression cassettes were constructed by fusing portions of the N terminus of the soybean HPPD to either DsRed2 or AcGFP1. The first fusion contained amino acid residues 1 to 42 of the long protein, while the second fusion contained residues 1 to 45 of the short HPPD protein (corresponding to residues 42–86 of the long protein). The third fusion contained the full 1 to 86 amino acids of the long HPPD protein. These cassettes, under the control of the Arabidopsis UBIQUITIN10 promoter, were used to transfect soybean seedling leaves. As shown in Figure 3, C to E, fluorescence was clearly visible in the chloroplasts of infected cells only when the marker gene was fused to amino acid residues 1 to 86. When the fusion was made with the shorter sequences of both proteins, fluorescence was visible only in the cytoplasm. The pattern of dual localization seen with the reporter constructs was confirmed by immunolocalization electron microscopy (Supplemental Fig. S3). Thus, the N-terminal 42 amino acids of the long protein are predicted to be a CTP, but to be functional, a longer sequence is required.

Although the N-terminal sequences of maize and soybean HPPD differ considerably (Fig. 3F), they are both able to target proteins in the heterologous species. Transient expression indicated that the long (1–86) HPPD protein N terminus targeted the marker protein to maize cell chloroplasts, while the protein variant with the shorter N termini delivered the protein to the cytosol (data not shown). Thus, the dicot dual-targeting region of soybean HPPD is able to function in monocot cells.

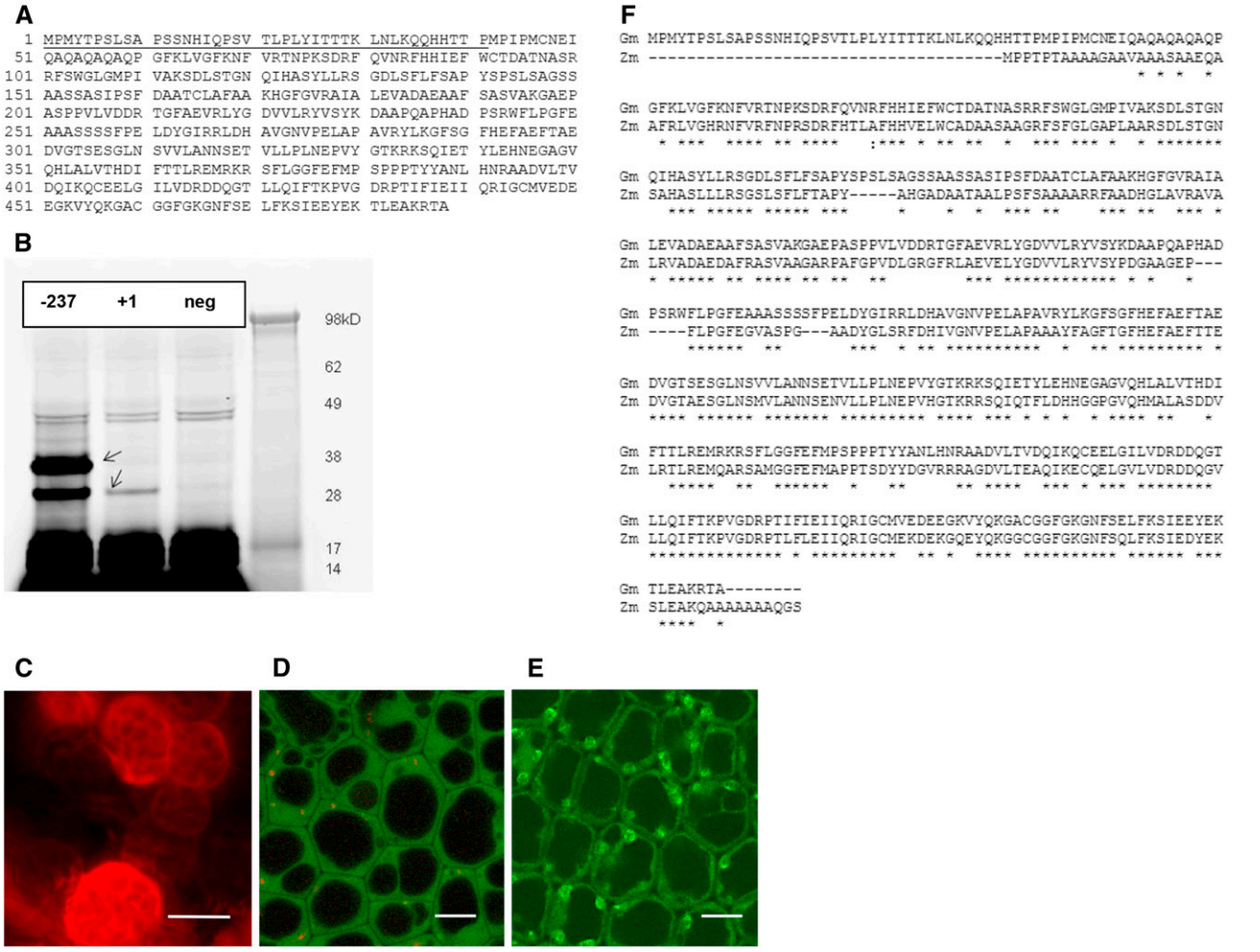

Figure 3. Genomic analysis of soybean HPPD. A, Soybean HPPD protein sequence with in-frame N-terminal extension (underlined). B, Protein polyacrylamide gel of in vitro transcription-translation products of the two (3′ truncated) HPPD transcripts. Predicted protein mass from −237 mRNA, 30.6 kD; +1 mRNA, 26 kD. C, Transient expression of the N-terminal fragment 1 to 42 fused to DsRed2 in soybean. D, Stable expression of the N-terminal fragment 42 to 86 fused to AcGFP1 in soybean. E, Stable expression of the N-terminal fragment 1 to 86 fused to AcGFP1 in soybean. Bars in C to E = 10 μm. F, Alignment of maize and soybean HPPD proteins. Asterisks indicate identity; the colon shows the fusion point of soybean to maize-insensitive HPPD proteins.

Because the reported HPPD sequences were misannotated for soybean, we examined available sequence data for Arabidopsis and another legume, *Medicago truncatula*. The Arabidopsis chromosome 1 HPPD gene NC_003070.9 (GenBank) encodes a 418-amino acid ORF with no upstream ORFs. The lack of N-terminal extension is punctuated by two in-frame stop codons 15 nucleotides upstream of the ATG start. On the other hand, a search of the *M. truncatula* genome returned a predicted HPPD gene located on chromosome 5 (NC_016411.1; GenBank), wherein the annotated predicted protein of 437 amino acids is preceded by a long ORF that could initiate at Met residues, adding 74 or 115 amino acids. The 74-amino acid N-terminal extension shows a very strong chloroplast localization score with PCLR (Schein et al., 2001), while the 115-amino acid extension did not. Functional analysis of the *M. truncatula* gene was not attempted. Dicot species appear to be either chloroplast targeted or not in a species-specific pattern that is still not clear. However, legumes may be unique in using the dual targeting approach.

Directed Evolution of the Maize HPPD Protein for Increased Insensitivity to Herbicide Inhibitors

All herbicidal inhibitors of HPPD are competitive inhibitors (Secor, 1994) and form a tight complex with the enzyme by the dual mechanisms of coordination to the active-site iron atom through a pair of keto oxygens and a π stack of the aromatic ring of the inhibitor between a pair of active-site Phe residues (Neidig et al., 2005). As a result, conventional 50% inhibition constant determinations are not able to distinguish differences in

binding affinity among various forms of HPPD and the inhibitor. All values will similarly approximate 50% of the enzyme concentration. To devise a parameter for detecting changes in inhibitor-binding affinity (K_D), we utilized the relationship between K_D and the rates of binding and release of inhibitor (I) to and from the enzyme (E):

$$E + I \underset{k_{OFF}}{\overset{k_{ON}}{\rightleftharpoons}} EI$$

At equilibrium, the rates of binding and release are equal. Thus:

$$k_{ON}[E][I] = k_{OFF}[EI]$$

Written as a dissociation, the equation can be rearranged to:

$$[E][I]/[EI] = k_{OFF}/k_{ON} = K_D$$

Higher K_D (reduced affinity or increased insensitivity) can be attained with a numerically smaller k_{ON}, a larger k_{OFF}, or both. To detect and quantify changes in k_{ON} and k_{OFF}, observations of the time course of an HPPD reaction as inhibitor binds to and inactivates the enzyme (k_{ON}) or is released from a preformed enzyme-inhibitor complex (k_{OFF}) were expressed as ON and OFF rate ratios, as described in Supplemental Figure S4. The ON and OFF rate ratios were multiplied, creating an insensitivity parameter that is a surrogate for K_D. K_D is expressed as k_{OFF}/k_{ON}, but because the ON rate ratio is an inverse parameter (the higher the value of the ON rate ratio, the lower the value of the represented phenomenon, k_{ON}), it is appropriate to multiply ON and OFF rate ratios. Another parameter, which quantifies the combined catalytic and insensitivity properties of the enzyme, is $k_{cat}/K_m \times$ ON rate ratio $\times$ OFF rate ratio, which is termed enzyme fitness. This parameter is intended to have a meaning similar to the commonly used expression $k_{cat}/K_m \times K_i$, where k_{cat} is the rate constant of the catalyzed reaction and K_i is the dissociation constant of the enzyme-inhibitor complex.

Directed evolution is an iterative process whereby beneficial diversity is discovered and iteratively recombined to evolve variants that achieve a desired protein engineering goal. Our goal was to create an HPPD enzyme that retained kinetic activity yet was insensitive to most or all HPPD-inhibiting herbicides. Characterization of the maize and soybean HPPD proteins showed that the former was 40-fold less sensitive to mesotrione than the latter (Table I). Therefore, we chose to improve the maize enzyme for use in soybean plants. Final evaluation of shuffled HPPD enzymes was carried out with multiple HPPD herbicides to select the most robust variant.

In the first six rounds, shuffled gene variant libraries were made based on the maize HPPD protein template using techniques including family shuffling, single-gene shuffling, back-crossing, and semisynthetic and synthetic shuffling (Zhang et al., 1997; Crameri et al., 1998; Ness et al., 2002). The amino acid diversity for those libraries originated from phylogenetic sequence diversity, random mutagenesis, site-directed mutagenesis, and structural features based on crystal structures of proteins in the Protein Data Bank (PDB; www.pdb.org/pdb/home/home.do). Typically, 4,000 to 5,000 variants per library were screened for kinetic and insensitivity parameters. Genes coding for shuffled variants of HPPD were expressed in *Escherichia coli*. Colonies with active HPPD enzyme cause the medium to turn brown due to the conversion of homogentisate to a brown ochronotic pigment (Zannoni et al., 1969). Proteins with the ability to turn the medium brown in the presence of 100 μM mesotrione in rounds 1 to 6 or tembotrione in rounds 7 and 8 were subjected to detailed analysis. Kinetic characteristics of k_{ON}, k_{OFF}, k_{cat}, and K_m were determined (Table I).

Saturation mutagenesis was used to discover functional diversity not available in the sequence database or accessed by other methods. As in all libraries, substitutions in the chloroplast-targeting amino terminus

Table I. *Kinetic activity and insensitivity parameters of purified evolved HPPD enzymes compared with the wild types from maize and soybean*

Insensitivity and fitness measurements are for the herbicidal compound mesotrione. Amino acid sequences are provided in Supplemental Figure S5.

HPPD Variant	Kinetic Parameters			Insensitivity Parameters				Fitness	
	k_{cat}	K_m	k_{cat}/K_m	ON Rate Ratio	OFF Rate Ratio	ON × OFF	Fold versus Maize Wild Type	ON × OFF × k_{cat}/K_m	Fold versus Maize Wild Type
	min^{-1}	μM							
Maize wild type	219	6.4	34.2	0.20	0.31	0.06	1	2.1	1
Soybean wild type	100	3.0	33.3	0.20	0.01	0.001	0.02	0.05	0.02
R1-1980	86	4.0	21.6	0.44	0.12	0.05	0.9	1.2	0.6
R2-1981	50	2.7	18.9	0.70	0.18	0.13	2.1	2.4	1.1
R3-1982	96	2.6	36.8	0.58	0.13	0.08	1.3	2.9	1.4
R4-1983	117	4.3	27.5	0.61	0.16	0.10	1.6	2.7	1.3
R5-9043	146	5.9	24.7	0.60	0.63	0.38	6.2	9.3	4.4
R6-9075	114	4.0	28.9	0.68	0.68	0.46	7.6	13.4	6.4
R7-9070	89	2.9	30.7	0.67	0.83	0.56	9.1	16.6	7.9
R8-1973	71	2.0	35.2	0.73	1.00	0.73	11.9	25.5	12.2

and the 14 positions that are within 4 Å of 2-[2-nitro-4-(trifluoromethyl)benzoyl]-cyclohexane-1,3-dione in the PDB 1T47 *Streptomyces avermitilis* structure (Brownlee et al., 2004) were avoided. The initial site saturation libraries and recombinant library of 19 novel substitutions at 14 sites, termed round 8, were screened for fitness with tembotrione.

The diversity of substitutions found in the improved HPPD enzymes of this study is listed in Supplemental Table S1. In many cases, a single substitution was identified, while at other positions, many neutral or beneficial substitutions were identified. Figure 4A illustrates the progression of desensitization to mesotrione from the wild type to the best variant that emerged from the round 8 library. Overall improvements of 12- and 35-fold for mesotrione and tembotrione, respectively, were achieved (Table I; Fig. 4B).

Because there are diverse chemotypes among the registered herbicidal inhibitors of HPPD, a commercially valuable trait should confer tolerance to most or all of these registered chemistries. To ensure that directed evolution met that criterion, parents for each successive library were tested for insensitivity to the other inhibitors shown in Figure 1B, using the same procedures as for mesotrione. The result was that improved insensitivity, and hence enzyme fitness, obtained by selection with mesotrione or tembotrione was accompanied by improved insensitivity to all other inhibitors (Fig. 4B).

Isolation and Characterization of the Soybean HPPD Promoter

To mimic the pattern of expression with regard to growth stage, tissue and subcellular location, and uncharacterized signaling cues, the transgene promoters were based on the native soybean HPPD promoter. Attempts to directly isolate or measure native HPPD protein accumulation indicated low abundance in leaves (data not shown). This was confirmed by EST analysis. Our premise was that preserving the native expression pattern for HPPD while substituting in the improved insensitive maize HPPD variant genes would confer robust herbicide tolerance with only moderately higher expression of the transgene relative to the native.

A 1,225-bp genomic sequence at the 5′ end of the soybean HPPD gene was isolated, sequenced, and subjected to promoter analysis using Promoter REAPer and Promoter Delineator (Simmons and Navarro Acevedo, 2010). Five putative TATA boxes, GTATAAATAA(TATA1), CCAATATATG(TATA2), CCTTATATATC(TATA3), TATATAATAA(TATA4), and GAATATAAG(TATA5), were identified as shown in Figure 5A. The ORF starting from the first ATG after TATA3 encodes the 449-amino acid short protein. TATA2 is within the long protein transcript, and TATA3 is embedded in the coding region for the long protein. Based on the known transcripts, TATA5 and TATA3 appear to be best situated for the long and short transcripts, respectively. Each is located approximately 35 nucleotides from the transcription initiation, as expected for eukaryotic promoters (Smale and Kadonaga, 2003). ORF analysis of the long transcript indicates a short ORF encoding seven amino acids starting at position −195. Downstream of this, the long ORF begins at position −99 and continues in frame comprising the short protein, which starts at +25. A schematic of the soybean HPPD promoter, transcripts, and translation products is shown in Figure 5B.

To evaluate the predicted TATA boxes for activity, 3′ deletions and various mutations of the promoter region were constructed and the fragments fused with DsRed2 for expression analysis using transient expression in bush bean leaf tissue. Deletion of a 613-bp DNA fragment upstream of the short protein transcription start site, including all five putative TATA boxes, resulted in the elimination of promoter activity. When TATA3 and the short transcript region were deleted with the DsRed2 initiating at the same position as the long protein, 90% of the full promoter region accumulation of DsRed2 was measured, showing the contribution of the upstream transcript. To eliminate translation of the long protein and leave only the contribution of the short protein, a stop codon was introduced upstream of the DsRed2

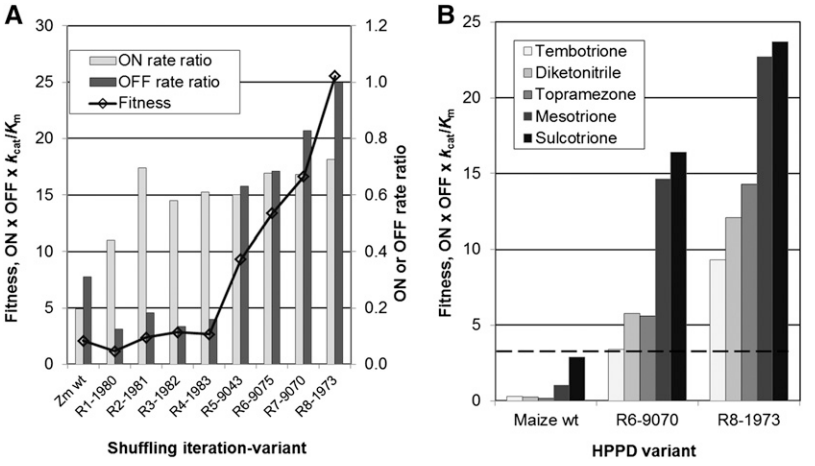

Figure 4. A, Progression of enzyme fitness for mesotrione with rounds of shuffling. Bars indicate ON and OFF rate ratios, the insensitivity parameters that are functions of the rate constants for association and dissociation of enzyme and inhibitor, respectively. Fitness is the product of k_{cat}/K_m and insensitivity parameters (ON rate ratio and OFF rate ratio) and approximates $k_{cat}/K_m \times K_i$. B, Selection for insensitivity to mesotrione or tembotrione resulted in cross-insensitivity to other herbicidal inhibitors. The dashed line is drawn at the fitness level that provided tolerance in soybean to twice the labeled field rate (for maize) of tembotrione in 2013 field trials.

protein, which replaced the short protein. Only the short transcript DsRed2 would be translated in this construct. The same amount of DsRed2 accumulated as with the previous vector. Thus, it appears that both transcripts are capable of supporting translation activity, but this activity is not additive. Total HPPD product from the native promoter could be regulated via competition for transcription and/or translation. Upstream ORFs have been shown to reduce both transcription and translation in plant genes (Saul et al., 2009). However, in this case, a mutation to eliminate the ATG start codon of the HPPD upstream ORF had no effect on DsRed2 expression compared with the unaltered promoter construct.

To create transgene expression cassettes for HPPD inhibitor herbicide tolerance in soybean, cassettes were constructed with the intention of maintaining the HPPD regulatory information while modestly increasing the expression level. In some cases, either TATA3 or TATA5 was replaced with a synthetic core promoter (SynII; Bowen et al., 2000) to drive the short or long transcripts at an increased level. DsRed2 fusion constructs with SynII exhibited 2- to 3-fold increased protein accumulation. Adding the 35S enhancer region (Ow et al., 1987) at the 5′ end of the altered promoter fragments or adding an enhancing region called Rsyn7, containing transcription factor motif sequences (Bowen et al., 2000), further increased expression. Plant transformation constructs were designed either with full-length shuffled maize HPPD in combination with promoters giving rise to only one transcript (e.g. Synthetic HPPD Promoter [SHP] 206:HPPD 9075) or with the N-terminal 86 amino acids of the long chloroplast targeting sequence of soybean followed by the conserved mature shuffled maize HPPD protein starting at amino acid 50 (e.g. SHP110e:HPPD Gm86:9075; Fig. 3F). The latter was designed to provide dual targeting of a highly insensitive HPPD enzyme. Final functional validation of the promoter/CTP/variant HPPD cassettes was by herbicide tolerance efficacy testing of transgenic soybean plants.

Herbicide Tolerance Conferred by Insensitive Maize HPPD in Soybean

Transgenic soybean events were created using particle bombardment of elite cultivar embryogenic callus cultures and selection with chlorsulfuron. T0 regenerated plants were acclimated to greenhouse conditions in soil

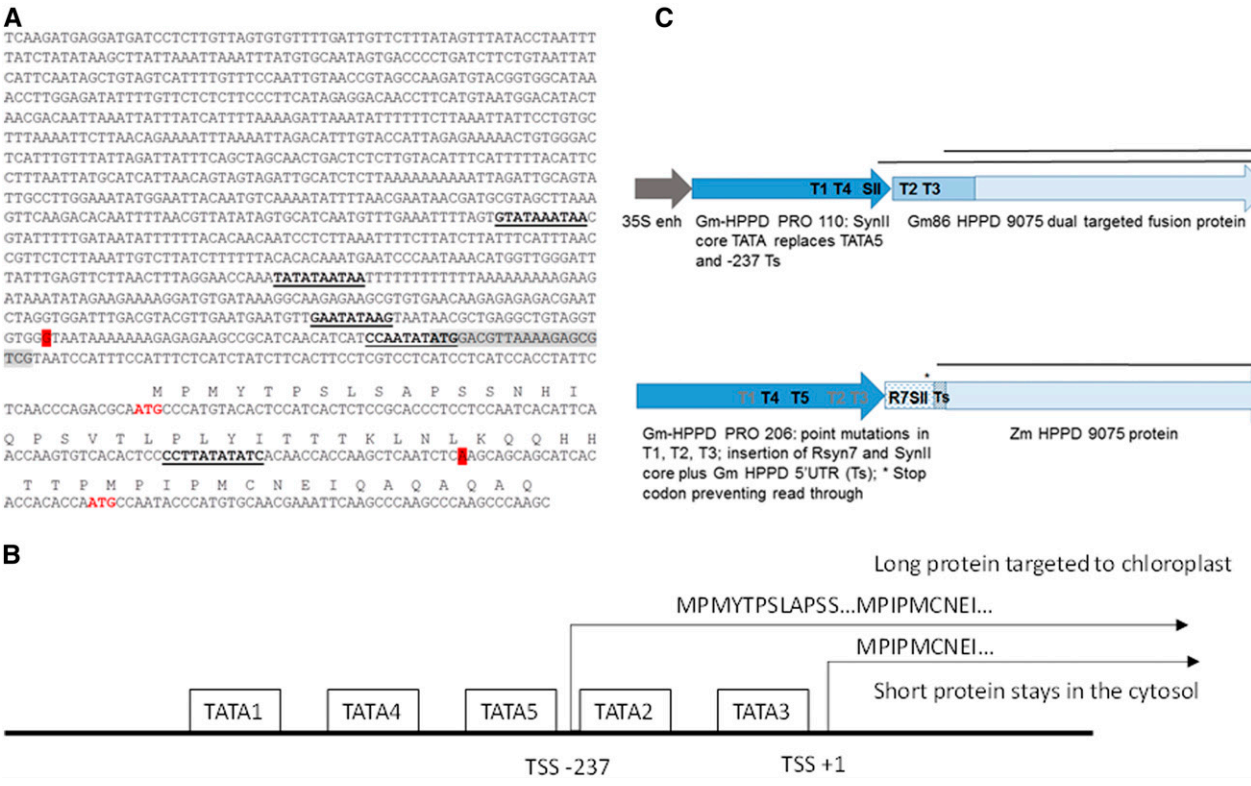

Figure 5. A, Upstream 1,225-bp soybean promoter sequence and N-terminal regions of the long and short HPPD proteins. Underlined bold denotes predicted TATA sequences, red boldface denotes Met initiation sites for long and short proteins, red background denotes actual transcription start sites at positions −237 and +1, and the gray box denotes the upstream ORF in the long transcript. B, Schematic of the soybean HPPD promoter and coding region. C, Schematics of example constructs SHP110e: HPPD Gm86:9075 and SHP206:HPPD 9075 used to create stably transformed soybean events. The amino acid sequence of round 6 HPPD 9075 is provided in Supplemental Figure S5.

for 2 weeks and sprayed with twice the labeled maize field rate (2×) of mesotrione. When sibling regenerants from the same event were available, the second plant was sprayed with 2× tembotrione. For each construct, approximately 30 events were created with one or two copies of the HPPD insert at a single locus. Events that showed 30% or less injury to 2× mesotrione and 2× tembotrione (on sibling plants) were retained. T0 plants were sampled for DNA analysis to verify single-copy inserts and for protein analysis to measure HPPD accumulation in young leaves. Plants were grown to maturity, and the T1 seeds obtained were sown in the greenhouse or the field. T1 plants were treated with 4× mesotrione and screened by PCR to identify homozygotes. Tolerant (at or below 30% injury) homozygous lines were grown and harvested for seed increase.

For positive control comparisons, the strong synthetic virus-based promoters SUP and SCP1 (defined in Bowen et al., 2000) were used to drive HPPD variants. Repeated occurrences of wrinkled- leaf and chlorotic- leaf phenotypes along with occasional sterility in the SUP and SCP1 events suggested that these promoters were not optimal for event production. Measurements of HPPD protein accumulation in young leaves of T0 plants revealed that the strong synthetic promoters accumulated HPPD protein at or above 10 mg g^{-1} of total soluble protein. The promoters derived from the soybean native HPPD promoter led to the accumulation of HPPD protein in tolerant events at levels in the range of 0.2 to 1 mg g^{-1} total soluble protein. All localization scenarios resulted in the production of some herbicide-tolerant events, of varying efficacy. Neither protein accumulation nor construct properties alone predicted greenhouse T0 efficacy results. In all cases, however, tolerance to mesotrione at the maize field rate was more easily achieved than tolerance to tembotrione.

Field tests in 2013 with homozygous lines expressing the round 6 desensitized HPPD variant 9075 showed that several events created were highly tolerant to mesotrione, tembotrione, and isoxaflutole at 2× or 4× treatment levels. Some transient injury was apparent, but by 14 d after treatment, the plants were almost completely recovered, as shown in Figure 6. Tabulated results for two different events are shown in Table II. Additional testing of these events and round 8 variant events in a variety of environments and in several genetic backgrounds is in progress.

DISCUSSION

In addition to a steadily increasing inventory of glyphosate-resistant weeds, there are documented cases of weeds, such as *Amaranthus* spp., that are resistant to multiple herbicides, including acetolactate synthase inhibitors, atrazine, protoporphyrinogen oxidase inhibitors, HPPD inhibitors, and glyphosate (Heap, 2014). With no new broad-spectrum herbicides on the horizon, it will be essential for farmers to adopt best management practices, such as knowing which weed species are in the fields and which herbicides will control them and using multiple herbicides with differing modes of action together or in the same season to prevent resistant weeds from reproducing (Norsworthy et al., 2012). The availability of robust herbicide tolerance traits to complement glyphosate will facilitate the practice of using multiple herbicides to control the emergence and spread of resistant weeds.

Our first step in developing HPPD-tolerant soybean was to understand the physiological nature of the HPPD pathway in soybean (Fig. 1A). HPPD catalyzes the conversion of HPP and molecular oxygen to homogentisate. Current evidence supports a pathway structure in which HPP is produced by an aminotransferase from Tyr, which in turn is produced from prephenate via arogenate (Tzin and Galili, 2010). Extensive genetic and biochemical data indicate that a complete pathway for the biosynthesis of the three aromatic amino acids exists in chloroplasts (Maeda and Dudareva, 2012). Likewise, the enzymes that convert homogentisate to plastoquinone and tocopherol are also plastidic (Ruiz-Sola and Rodriguez-Conception, 2012).

Given a chloroplast localization of Tyr synthesis and homogentisate utilization, one might anticipate that

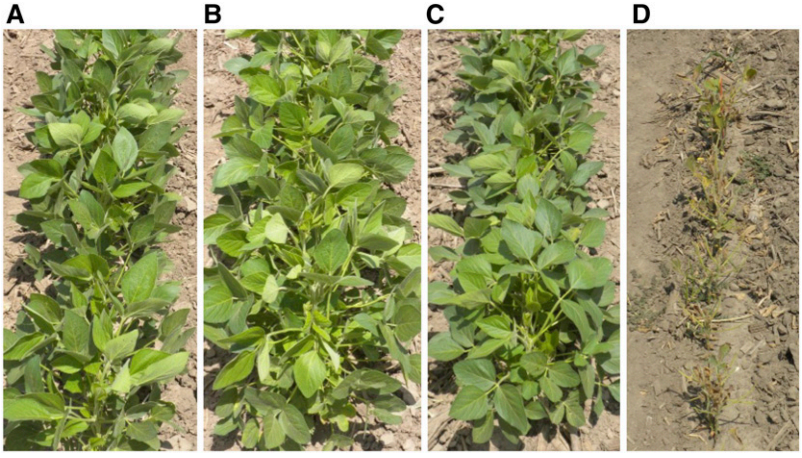

Figure 6. Field trial with herbicide-tolerant transgenic soybean events treated with 2× the maize field rate of tembotrione 14 d after treatment. A, T3 generation homozygous plants expressing promoter SHP206 and full-length maize HPPD variant round 6 9075. B, T3 generation homozygous plants expressing 35S-enhanced promoter SHP110 with HPPD Gm86:9075. C, Nontransgenic unsprayed control. D, Nontransgenic sprayed control. Treatment was as described in Table II.

Table II. *Transgenic soybean plants expressing insensitive HPPD variant constructs showing tolerance to three different HPPD-inhibitor herbicides in the field*

Seeds were homozygous for single-copy inserts in elite genetic background. The visual rating scale was 0% (no injury) to 100% (dead), with an average of three plots. DAT, Days after treatment; 2× and 4×, treatment levels. All treatments were sprayed at the V4 stage and included 0.25% (v/v) nonionic surfactant and 9.6 g L^{-1} ammonium sulfate.

Event Cassette	DAT	Visual Rating				
		Isoxaflutole[a]		Mesotrione[b]		Tembotrione[c]
		2×	4×	2×	4×	2×
		%				
No transgene	3	26.7	28.3	33.3	33.3	28.3
No transgene	7	61.7	63.3	71.7	71.7	71.7
No transgene	14	81.7	85.0	81.7	86.7	90.0
SHP206:HPPD 9075	3	1.0	3.0	10.0	20.0	8.0
SHP206:HPPD 9075	7	0.7	1.0	1.7	8.3	4.3
SHP206:HPPD 9075	14	0.0	0.0	0.0	3.3	1.0
SHP110e:HPPD Gm86:9075	3	0.0	2.0	13.0	20.0	13.0
SHP110e:HPPD Gm86:9075	7	0.0	0.0	3.7	11.7	19.0
SHP110e:HPPD Gm86:9075	14	0.0	0.0	0.0	0.7	4.0

[a]Isoxaflutole, 1× = 67 g active ingredient (ai) ha^{-1}. [b]Mesotrione, 1× = 118 g ai ha^{-1}. [c]Tembotrione, 1× = 90 g ai ha^{-1}.

Tyr aminotransferase and HPPD would be found in the chloroplast. Data on Tyr aminotransferase are sparse, but it was shown recently that Arabidopsis gene locus At5g53970 encodes a specific and catalytically proficient Tyr:2-ketoglutarate aminotransferase that contributes a major but not exclusive portion of that activity (Riewe et al., 2012). Localization was not determined in that study. However, a petunia (*Petunia hybrida*) paralog of At5g53970 codes for a cytosolic enzyme that catalyzes the transamination of Tyr to HPP with phenylpyruvate as the acceptor substrate, providing for the special need for Phe in the petals as a precursor for aroma compounds (Yoo et al., 2013). HPP can also be made directly from prephenate, catalyzed by prephenate dehydrogenase (PDH). Although lacking in 10 nonlegume species tested, PDH activity was detected in various legumes, including soybean (Siehl, 1999). PDH activity in soybean (and *Medicago* spp.) was recently confirmed, genes identified, and the enzyme shown to be located in the cytosol (Schenck et al., 2014).

Our results with HPPD add to what appears to be a species-dependent variety of localization patterns. It was reported previously that Arabidopsis and *Brassica* spp. do not have predicted CTPs, while cotton and tomato do. Our analysis of the maize sequence did not predict a CTP but did predict a CTP for a previously unrecognized N-terminal extension of HPPD from soybean. Plant targeting peptides are very heterogenous, and different prediction programs often give conflicting results (Bruce, 2001; Jarvis, 2008). Thus, functional analysis was needed to validate the in planta localization of HPPD for each species. In the case of the maize HPPD, the N-terminal 50 amino acids were necessary and sufficient for chloroplast targeting in monocot and dicot cells. The soybean HPPD localization was more complex. We found two major ESTs with the long transcript giving rise to a protein both predicted and validated as capable of being translocated to the chloroplast, while the short transcript supported translation of a shorter protein that accumulated in the cytosol.

Why would the HPPD enzymatic step ever be localized in the cytosol? In theory, soybean and other legumes have a cytosolic minipathway that includes the cytosolic isozymes of chorismate mutase, PDH, and the short translation product of HPPD (Fig. 1A). While PDH bypasses prephenate aminotransferase, arogenate dehydrogenase, and Tyr aminotransferase, one still must postulate that the substrate (chorismate) and product (homogentisate) of the cytosolic minipathway must be transported across the chloroplast membrane. It is possible that the dual localization of HPPD is unique to legumes. Analysis of the *M. truncatula* genome sequence around the HPPD gene revealed that this legume species also has an N-terminal ORF extension that contains a predicted CTP. What is not clear is why Arabidopsis and some other nonlegumes would encode only cytosolic HPPD (Garcia et al., 1997, 1999). Perhaps the movement of homogentisate into the chloroplast serves as a regulatory step for the plastoquinone and tocopherol pathways.

HPPD is the second step in the Tyr degradation pathway. Genes for all the subsequent pathway steps have been identified in Arabidopsis, shown to be expressed, and the encoded enzymes shown to be fully functional (Dixon and Edwards, 2006). Interestingly, just as deficiency in fumarylacetoacetate hydrolase, the ultimate step in the pathway, is a lethal disorder in animals, disruption of the same enzyme in Arabidopsis causes spontaneous cell death (Han et al., 2013). Although not investigated, overloading the Tyr degradation pathway may be a causal contributor to the negative phenotype seen when HPPD is expressed far above native levels.

Instead of relying on high overexpression of a transgene, we sought to enhance efficacy by creating highly insensitive HPPD variants. Despite the availability of structural analysis and rational design, the greatest gains in evolving the HPPD enzyme for inhibitor insensitivity were achieved with the introduction of primarily conservative diversity present in related sequences. Introduction of nonnaturally occurring diversity through saturation mutagenesis revealed novel beneficial mutations that were not available in the natural diversity. Assembling them in random combinations provided a further 3-fold improved fitness compared with the best round 6 variant. The variant with the highest fitness parameter, R8-1973, had 26 amino acid substitutions relative to native maize HPPD. The substitutions were distributed throughout the amino acid sequence and did not involve an amino acid with any reported role in catalytic function (Raspail et al., 2011). The evolution of improved function appeared to occur through the accumulated effect of many small changes outside of the active site that influence the catalytic properties of the enzyme in a manner that is not obvious upon inspection of the structure. We reached a similar conclusion after evolving a microbial acetyltransferase for activity with glyphosate (Siehl et al., 2007). Although desensitization to herbicidal inhibitors was associated with a drop in k_{cat} from approximately 200 min^{-1} to 70 to 80 min^{-1}, nominal catalytic efficiency (k_{cat}/K_m) was preserved due to a drop in K_m from 6 μM to 2 to 3 μM (Table I).

A component of the effective management of herbicide-resistant weeds is the use of compounds with various modes or sites of action within a program of best management practices. Adding HPPD inhibitors to the panel of available herbicides will allow growers to expand the choices of weed control chemistry they can use in soybean and other dicot crops. We believe that this work provides a viable candidate for a robust HPPD tolerance trait that should provide functional resistance to a broad range of HPPD inhibitor chemotypes.

MATERIALS AND METHODS

Genomic and Transcript Analysis

A synthetic maize (*Zea mays*) wild-type HPPD complementary DNA (NCBI reference sequence NM_001112312.1) was assembled from commercially synthesized oligonucleotides. During the synthesis of the gene, an *Nco*I restriction site was engineered into the start of the sequence to facilitate cloning. The change of codon ATGCCC to ATGGGT resulted in the substitution of Gly for Pro at position 2. An EST (sgc5c.pk001.j9) coding for soybean (*Glycine max*) HPPD was identified from a DuPont-Pioneer proprietary soybean EST database using conventional bioinformatic tools including BLAST of the HPPD sequence described by Cahoon and Coughlan (2007). Using this soybean HPPD coding sequence as query, Pioneer Unigene PSO409914 was identified. An approximately 2-kb genomic sequence upstream of the EST was then identified from the genome assembly database. PCR primers (forward primer 5′-GCAAGTATTTCAATACAATAGC-3′ and reverse primer 5′-GTTATCTGATATGATGTTGC-3′) were used to amplify the HPPD locus from genomic DNA isolated from an elite soybean variety and the common Jack variety, following protocols for the isolation of plant genomic DNA (Qiagen). PCR reaction parameters were as follows: cycle 1, 94°C for 2 min; cycles 2 to 30, 94°C for 30 s, 65°C for 1 min, and 72°C for 5 min; cycle 31, 72°C for 10 min. A proofreading DNA polymerase, *pfu* Turbo (Stratagene), was used for PCR amplification. A 4,306-bp fragment and a 4,310-bp fragment were obtained from elite and Jack, respectively. These fragments were cloned into Zero blunt TOPO PCR cloning vectors (Invitrogen) and fully sequenced. Each locus comprises 3′ sequences, the HPPD coding region, and upstream genomic sequence. The loci are highly conserved, with an overall 99% sequence identity at the nucleotide level.

5′ RACE was used to validate transcription start sites for the native HPPD promoter using total RNA extracted from young elite soybean leaves and the First Choice RLM-RACE kit (Ambion) according to the manufacturer's protocol. Total RNA was isolated with the Qiagen RNeasy mini kit. Linked transcription-translation was performed with a Promega wheat germ kit, using 3′ truncated soybean HPPD transcription vectors, and the products were analyzed by SDS gel electrophoresis (8%–12% gradient; Invitrogen).

Expression Vectors for Localization Microscopy and Promoter Analysis

Monocot transient expression vectors were made with DNA encoding N-terminal fragments of monocot HPPD proteins, the soybean HPPD protein, or the synthetic monocot consensus peptide fused to the gene coding for DsRed2 and C3GFP (Clontech) and inserted into a binary expression vector under the control of the maize Rubisco activase promoter (Liu et al., 1996) or the Arabidopsis (*Arabidopsis thaliana*) UBIQUITIN10 promoter (Norris, et al., 1993) and terminated with the potato (*Solanum tuberosum*) proteinase inhibitor II terminator region (An et al., 1989) with a hygromycin selection cassette. The vector also contained an untargeted *Zoanthus* sp. Green cassette to provide cytoplasmic contrast and a kanamycin selection cassette. All genes were between the left and right border sequences of *Agrobacterium tumefaciens* transfer DNA. A positive control vector was identical except that the insert was DsRed2 fused to the CTP of Arabidopsis Rubisco activase, while a negative control was DsRed2 with no targeting sequence.

A second set of fluorescent vectors were similarly made with an *AcGFP1* gene and inserted into a binary expression vector under the control of the Arabidopsis UBIQUITIN10 promoter (Norris et al., 1993) and terminated with the soybean Kunitz trypsin inhibitor 3 terminator region (NCBI accession no. S45092). Such vectors were used for either stable or transient gene expression in dicot plant cells. Fusions for testing the soybean CTP function contained the sequence- encoding amino acid residues 1 to 42, 42 to 86, or 1 to 86 of the long soybean HPPD protein. A positive control vector was identical except that the AcGFP1 coding region was fused to sequences encoding the 6H1 synthetic CTP (Lassner and Wilkinson, 2008), while a negative control was AcGFP1 with no targeting sequence.

Cassettes for testing the transient expression of promoters were similar to the DsRed2 N-terminal test vectors except that soybean HPPD promoter-derived fragments replaced the Rubisco and UBIQUITIN10 promoters. A 2,061-bp fragment comprising the native HPPD promoter of elite soybean was created from the upstream genomic sequence. The PCR with forward primer hp0234 (5′-GTTTT CCGCGGG TGTTGATCC-3′) and reverse primer hp2296 (5′-TCATT GGTACC TGGTGTGGTGTGATGCTGC-3′) introduced *Sac*II and *Kpn*I restriction sites. This fragment was digested with restriction enzymes *Sac*II and *Kpn*I and ligated to a DsRed2 marker gene to form the native soybean HPPD promoter expression cassette. Introduction of the *Kpn*I site between the promoter fragments and DsRed2 resulted in the introduction of a two-amino acid linker (GGTACC, Gly-Thr) in the fusion proteins containing the long protein CTP region.

The 1,225-bp genomic sequence at the 3′ end of the promoter fragment was subjected to in silico promoter analysis using Promoter REAPer and Promoter Delineator (Simmons and Navarro Acevedo, 2010). Genomic sequences from other species including Arabidopsis, *Medicago truncatula*, *Populus trichocarpa*, *Brassica rapa*, *Vitis vinifera*, and the monocot sorghum (*Sorghum bicolor*) were included for comparison in this analysis. With the program Promoter REAPer, regions were identified in the soybean HPPD promoter that are predicted to be important for its activity based on the sequence conservation of a set of DNA motifs across the seven plant species. To evaluate the predicted TATA boxes in promoter activity, a deletion series was created with the 2,061-bp template using PCR with forward primer hp0234 (5′-GTTTTCCGCGGGTGTTGATCC-3′) and the reverse primers hp2154 (5′-AGCATGGTACCTTGCGTCTGGGTTGAG-3′), hp2048 (5′-ATCTGGTACCTGATGTTGATGCGGC-3′), hp1962 (5′-AGGAGGTACCGTCAAATCCACCTAG-3′), hp1791 (5′-AGCCTGGTACCTTGTGTGTAAAAAAGATAAGAC-3′), and hp1663 (5′-TCCTTGGTACCTGATGCACTATATAACG-3′). Single or triple mutations in the putative TATA boxes were created using site-directed mutagenesis (QuickChange; Stratagene). The resultant

deletion and mutated promoter fragments were fused with DsRed2 to create cassettes for the analysis of expression activity in agroinfiltrated leaf tissues.

To create synthetic promoters based on the soybean HPPD promoter, synthetic elements based on the SynII core promoter and the Rsyn7 transcription factor-binding sequence (Bowen et al., 2000), each flanked by restriction sites *Xho*I and *Kpn*I, were synthesized and ligated with the 3′ ends of HPPD promoter-derived DNA fragments. SHP110e contains a cauliflower mosaic virus 35S enhancer (Ow et al., 1987) at the 5′ end of the promoter fragment and a partial SynII core sequence inserted in place of TATA5. This promoter allows dual targeted proteins to be created with soybean-maize HPPD fusion proteins. SHP206 has point mutations in each of TATA1, TATA2, and TATA3. After the mutated TATA3 are the Rsyn7 enhancer and the SynII core followed by the 45-bp 5′ untranslated region and the transcription start site of the native soybean gene. An in-frame stop codon prevents read through from upstream transcripts.

Marker Gene Expression and Fluorescence Measurements

All seedling plants were grown in growth chambers with 16 h of light at 375 to 450 μmol m^{-2} s^{-1}, 26°C day, and 22°C night. Expression plasmids for localization studies were transformed into *A. tumefaciens* AGL-1 via electroporation according to Shen and Forde (1989), and agroinfiltration (Kapila et al., 1997) was used to introduce the constructs into plant cells. *A. tumefaciens* cultures were grown overnight in Luria-Bertani medium with 40 mg L^{-1} kanamycin and a working suspension normalized to an optical density (OD) at 600 nm of 1 in 10 mM $MgSO_4$, 400 μm acetosyringone, and 1 mM dithiothreitol (DTT). Leaves of 3-week-old maize or sorghum seedlings were infiltrated with the *A. tumefaciens* and examined by epifluorescence microscopy of hand sections 2 d later (Nikon Eclipse 80i microscope, with a 40×/0.75 Plan Fluor Ph2 DLL objective through a TRITC HQR-Nikon 96321 filter) to visualize DsRed2. Images were captured with a Nikon Digital DS-5M camera and ACT-2U version 1.11.22.156 image-capture software. Exposure times of 1.5 to 3 s were used for all fluorescent image captures with a sharpness setting of 3. Infiltrated leaf samples were derived from plants of uniform developmental stage grown under the same conditions. Leaves of 4-week-old tobacco (*Nicotiana benthamiana*), 8-d-old bush bean (*Phaseolus vulgaris* variety Shade), and 10-d-old soybean seedlings were infiltrated with the *A. tumefaciens* and examined by epifluorescence microscopy of hand sections 4 to 5 d later using a Nikon Eclipse 80i microscope and a narrow band-pass GFP filter set.

Qualitative assessment of protein localization via bombardment with DsRed2 was determined by visually inspecting treated samples with a stereofluorescence microscope (Leica Microsystems; M165 FC with DsRed2 filter set no. 10447412) and acquiring images (Leica Microsystems; DFC300 FX R2) of representative examples at fixed exposure times. Initial examination of maize tissues expressing C3GFP or soybean tissues expressing AcGFP1 was conducted at approximately 24 h after bombardment with a Lumar fluorescence stereomicroscope (Carl Zeiss) equipped with both UV light-exciting (Zeiss Set 01) and red light-emitting (Zeiss Set 43 HE) filter sets to image the GFP and DsRed2, respectively. GFP fluorescence was captured using a 488-nm argon laser for excitation laser and a 500- to 550-nm band-pass emission filter. DsRed fluorescence was imaged using a 561-nm diode laser for excitation and a 575- to 615-nm band-pass emission filter. Chlorophyll fluorescence was captured by combining a 561-nm excitation and a 650- to 710-nm band-pass emission filter. AcGFP expression in stably transformed soybean seedlings was imaged with the confocal microscope in an identical fashion to bombarded tissues.

A. tumefaciens strains expressing plasmids for promoter characterization were infiltrated into bush bean leaves. Relative promoter strength was determined by quantitative measurement of the red fluorescence generated from expressed DsRed2 protein in infiltrated leaf tissues. Red fluorescence from 50 μg of protein extracted from infiltrated leaf discs was quantified using a Typhoon Trio+ Variable Mode Imager. Infiltration experiments for each construct were repeated at least three times. The background red fluorescence detected in leaves infiltrated with the negative control vector consisting of the double-enhanced version of the mirabilis mosaic virus promoter (Dey and Maiti, 1999) driving a GUS reporter was subtracted for data normalization. The DsRed2 readouts were used to calculate the level of DsRed2 from each construct relative to the DsRed2 expressed from the full native promoter construct (2,061 nucleotides 5′ to the ATG of the short protein), which was set to 100%. Up to 30 leaf discs infected with the same culture were pooled for analysis. Each pool of infiltrated leaf samples (about 260 mg fresh weight) represented tissue equally derived from 15 plants of uniform developmental stage.

HPPD Expression, Purification, and Kinetic Analysis

Wild-type and shuffled variant genes were cloned into a modified version of pET24a(+) (Novagen), which places six His residues at the N terminus of the expressed protein. Vectors were electroporated into *Escherichia coli* host strain BL21(DE3). Cells were grown at 30°C in rich medium such as 2× yeast extract tryptone containing the selection antibiotic kanamycin. At OD_{600} of about 0.6, isopropylthio-β-galactoside was added to 0.2 mM, the temperature was reduced to 16°C, and growth was continued for another 24 h. Cells were harvested by centrifugation and stored at −80°C. Cell pellets were lysed in BPER (Thermo Scientific) protein extraction reagent containing 0.2 mg mL^{-1} lysozyme, 1 mM DTT, bacterial protease inhibitor cocktail (Sigma-Aldrich), and endonuclease. Insoluble cellular debris was removed by centrifugation. HPPD protein was purified from the soluble protein solution by affinity chromatography on the nickel form of nitrilotriacetic acid resin (Qiagen). Protein concentrations were determined by the Bradford method, as supplied by Bio-Rad.

HPPD activity was detected through conversion of its product homogentisate to maleylacetoacetate, catalyzed by homogentisate dioxygenase from *Pseudomonas aeruginosa* (Amaya et al., 2004; generously provided by Dr. Graham Moran). The extinction at 320 nm was measured at 14.7 OD M^{-1} cm^{-1}. The homogentisate dioxygenase gene was expressed in *E. coli* strain BL21(DE3), and the protein was produced by methods similar to those described for HPPD. The purified enzyme had a K_m for homogentisate of 23 μM and a k_{cat} of 100 s^{-1}, parameters suitable for its use as a coupling enzyme.

HPPD activity was measured by placing a 6-μL aliquot of the substrate HPP at 50 times the desired final concentration into the wells of a low UV light-absorbing assay plate. Reactions were started by adding 294 μL of a mixture containing 25 mM HEPES, pH 7, 2 mM ascorbate, 10 μM $FeSO_4$, 1 to 100 μM HPP, 50 nM homogentisate dioxygenase, and 5 to 240 nM HPPD. A_{320} was monitored continuously in a plate-reading spectrophotometer (Spectramax; Molecular Devices). Catalytic performance was assessed by determining the substrate saturation parameters. The Michaelis-Menten kinetics protocol of the Spectramax software was customized for HPP concentrations ranging from 3.33 to 100 μM, or up to 1 mM if required. The software returned values of K_m and V_{max} using the Lineweaver-Burk transformation of the Michaelis-Menten equation.

To detect changes in ON and OFF rates, we observed the time course of an HPPD reaction as inhibitor binds to and inactivates the enzyme (k_{ON}) or is released from a preformed enzyme-inhibitor complex (k_{OFF}). In practice, a quantitative indicator of k_{ON} was obtained by monitoring the time courses of HPPD reactions containing 60 or 120 nM HPPD and 100 μM HPP in the presence and absence of 4 μM inhibitor (e.g. mesotrione). The ratio of the reaction rate with inhibitor to that without inhibitor during the 70- to 90-s interval of the reaction was termed the ON rate ratio.

A quantitative indicator of k_{OFF} was obtained by observing the time course of an HPPD reaction as inhibitor is released from a preformed enzyme-inhibitor complex. HPPD and inhibitor were incubated together at concentrations of 7.2 and 8 μM, respectively. Incubations with the same concentrations of enzyme but no inhibitor were done in parallel. After 1 h at room temperature, 5 to 10 μL of the enzyme-inhibitor complex was dispensed into the wells of the assay plate. Reactions were started with the addition of 290 to 295 μL of 25 mM HEPES, pH 7, 2 mM ascorbate, 10 μM $FeSO_4$, 100 μM HPP, and 50 nM homogentisate dioxygenase. The reactions were monitored at 320 nm for 12 min. Reaction velocity accelerated as inhibitor was released from the enzyme until a steady state was reached, during which the reaction velocity was constant. The ratio of the steady-state rate in mixtures containing mesotrione (or other herbicidal inhibitor) to the initial velocity of mixtures lacking inhibitor was termed the OFF rate ratio.

The diketonitrile form of isoxaflutole was synthesized by DuPont chemists. All other inhibitors were obtained from Sigma-Aldrich.

HPPD Protein Detection in Planta

HPPD protein concentration in young soybean leaves was measured using liquid chromatography-tandem mass spectrometry according to Hu and Owens (2011) with some modifications. Leaf samples were collected from the youngest expanded trifoliate leaf. Total extracted protein samples were normalized to 0.8 μg μL^{-1}. Sample extracts (50 μL) used for analysis and purified HPPD protein standards were spiked into 50-μL negative tissue extracts for standard curves. Samples were heated for 15 min at 95°C, and 80 μL of digestion buffer (100 mM ammonium bicarbonate with 0.05% [v/v] Tween 20) was added. The samples were reduced with 6 μL of 0.25 M DTT at 50°C for 30 min and then alkylated with 6 μL of 0.3 M iodoacetamide at room temperature, in the dark, for 30 min. Samples were digested with trypsin (1 μg in 10 μL)

and acidified. Internal standard (10 μL of peptide SIEDYEK, where K was labeled with stable isotopes ^{13}C and ^{15}N) was added. HPPD protein (10-μL injection) was quantified by its signature tryptic peptide SIEDYEK using a Waters ultra-performance liquid chromatography device coupled with the AB SCIEX QTRAP 4000 or 5500. Liquid chromatography was run with a linear gradient of 5% to 16% (v/v) 0.1% formic acid in acetonitrile over 2.5 min. Fragmentation transitions of 882.6 to 682.3 D and 890.6 to 690.3 D were monitored for peptide SIEDYEK and its internal standard peptide, respectively. Chromatogram peak area ratios to the corresponding internal standard were plotted against protein concentrations. The lower limit of quantification for HPPD by liquid chromatography-tandem mass spectrometry was 25 $\mu g\ g^{-1}$ of total extracted proteins.

Stable Soybean Transformation and Herbicide Testing

Soybean plants expressing HPPD transgenes or marker genes were produced using the method of particle gun bombardment (Klein et al., 1987) using a DuPont Biolistic PDS1000/He instrument. A selectable marker used to facilitate soybean transformation was a chimeric gene composed of the *S*-adenosyl-Met synthase promoter (Falco and Li, 2010) from soybean, a highly resistant allele of soybean acetolactate synthase (Bedbrook et al., 1997), and the native soybean acetolactate synthase terminator region. The selection agent used during the transformation process was chlorsulfuron. HPPD cassettes comprised a synthetic constitutive promoter (Bowen et al., 2000) or the soybean HPPD-derived promoters, an insensitive HPPD variant, and an Arabidopsis UBIQUITIN3 gene terminator (Callis et al., 1995). Bombardments were carried out with linear DNA fragments purified away from any bacterial vector DNA. The selectable marker gene cassette was in the same DNA fragment as the HPPD cassette. In some cases, the characterized CTP sequences 6H1 (Lassner and Wilkinson, 2008) and the Arabidopsis Rubisco large subunit CTP (Lee et al., 2006) were fused to a truncated maize HPPD variant. Bombarded soybean embryogenic suspension tissue was cultured for 1 week in the absence of selection agent and then placed in liquid selection medium for 6 weeks. Putative transgenic suspension tissue was sampled for PCR analysis to determine the presence of the HPPD gene. Putative transgenic suspension culture tissue was maintained in selection medium for 3 weeks to obtain enough tissue for plant regeneration. Suspension tissue was matured for 4 weeks using standard procedures; matured somatic embryos were desiccated for 4 to 7 d and then placed on germination induction medium for 2 to 4 weeks. Germinated plantlets were transferred to soil in cell pack trays for 3 weeks for acclimatization. Plantlets were potted to 10-inch pots in the greenhouse for evaluation of herbicide resistance. Metal halide lights with 160 $\mu E\ m^{-2}\ s^{-1}$ photosynthetically active radiation supplemented natural intensity during a 16-h photoperiod when light intensity was less than 500 $\mu E\ m^{-2}\ s^{-1}$. Day temperature was 28°C ± 2°C, and night temperature was 22°C ± 2°C. Relative humidity ranged from 50% to 90%.

T0 plants with HPPD transgenes were grown to the V2 to V8 growth stage and then sprayed in a chamber with commercial mesotrione (Callisto; Syngenta) formulation at a rate of 210 g ai ha^{-1} (two times the labeled rate for maize in the field). All mesotrione treatments were applied with 0.25% nonionic surfactant (Induce; Helena Chemical) and 1% ammonium sulfate in a spray volume of 374 L ha^{-1}. Individual plants were compared with untreated plants of similar genetic background, evaluated for herbicide response at 8 d after treatment, and assigned a visual response rating from 0% (no effect) to 100% (dead plant). Sibling plants were similarly evaluated with tembotrione (Laudis; Bayer Crop Science) at 93 g ai ha^{-1}. In the T0 generation, plants that had improved tolerance compared with controls based upon low injury scores (30% or less) were advanced for more extensive herbicide testing.

T1 plants were evaluated for zygosity via quantitative PCR. Homozygous single-locus transgenic plants and their corresponding null segregants were identified, and T2 true-breeding seed was obtained from each. Plants were grown to the V1 to V2 growth stage and then sprayed with the commercial formulation of mesotrione at 420 g ai ha^{-1} as described for the T0 stage.

Homozygous T3 generation seeds were planted in short rows in Johnston, IA, at a DuPont Pioneer regulated field location. Herbicides were applied at the V4 stage with a backpack sprayer in a spray volume of 140 L ha^{-1} at two or four times the labeled rates for maize in the field, which are as follows: mesotrione, 118 g ai ha^{-1}; tembotrione, 90 g ai ha^{-1}; and isoxaflutole, 67 g ai ha^{-1}. All treatments included 0.25% (v/v) nonionic surfactant and 9.6 g L^{-1} ammonium sulfate. As negative controls, rows of nontransformed plants of the same variety were sprayed at the same rates. Positive control rows received no spray. Visual injury was rated at 3, 7, and 14 d after treatment.

The sequence of the N-terminally extended soybean HPPD gene was deposited in GenBank with the accession number KM460829.

Supplemental Data

The following materials are available in the online version of this article.

Supplemental Figure S1. Immunolocalization of native HPPD in maize leaf shows label only in chloroplasts.

Supplemental Figure S2. The N-terminal 50 amino acids of maize HPPD directs fluorescent protein to the chloroplasts of maize leaf guard cells.

Supplemental Figure S3. Immunolocalization electron microscopy of HPPD in soybean cotyledons shows label in chloroplasts and cytoplasm.

Supplemental Figure S4. Indirect measurement of the rates of association and dissociation of inhibitors and HPPD.

Supplemental Figure S5. Amino acid sequences of the wild type and shuffled variants of maize HPPD characterized in Tables I and II and Figures 4 and 6.

Supplemental Table S1. Chart of diversity contributing to the improvement of insensitive maize HPPD.

ACKNOWLEDGMENTS

We thank Dr. Graham Moran (University of Wisconsin, Milwaukee) for generously providing a clone of *P. aeruginosa* homogentisate dioxygenase, Dr. Zhenglin Hou (DuPont Pioneer) for providing models of maize HPPD (based on PDB 1SP8) ligated with various inhibitors, Sean Bertain (DuPont Pioneer) for helpful consultation, and Dr. Hiroshi Maeda (University of Wisconsin, Madison) for data on soybean PDH prior to publication.

Received July 21, 2014; accepted August 23, 2014; published September 5, 2014.

LITERATURE CITED

Amaya AA, Brzezinski KT, Farrington N, Moran GR (2004) Kinetic analysis of human homogentisate 1,2-dioxygenase. Arch Biochem Biophys **421:** 135–142

An G, Mitra A, Choi HK, Costa MA, An K, Thornburg RW, Ryan CA (1989) Functional analysis of the 3′ control region of the potato wound-inducible proteinase inhibitor II gene. Plant Cell **1:** 115–122

APHIS (2009) Petition (09-328-01p) for determination of non-regulated status of event FG72 soybean Bayer CropScience LP and MS Technologies LLC. http://www.aphis.usda.gov/brs/aphisdocs/09_32801p_fpra.pdf

APHIS (2012) Revised petition (12-215-01p) for determination of non-regulated status for herbicide-tolerant event SYHT0H2 Soybean Syngenta Seeds Inc and Bayer CropScience AG. http://www.aphis.usda.gov/brs/aphisdocs/12_21501p_Syngenta_Submitted_ER.pdf

Bedbrook JR, Chaleff RS, Falco SC, Mazur BJ, Somerville CR, Yadav NS, inventors. February 25, 1997. Nucleic acid fragment encoding herbicide resistant plant acetolactate synthase. US Patent No. 5,605,011

Blum T, Briesemeister S, Kohlbacher O (2009) MultiLoc2: integrating phylogeny and Gene Ontology terms improves subcellular protein localization prediction. BMC Bioinformatics **10:** 274

Bowen BA, Bruce WB, Lu G, Sims LE, Tagliani LA, inventors. June 6, 2000. Synthetic promoters. US Patent No. 6,072,050

Brownlee JM, Johnson-Winters K, Harrison DHT, Moran GR (2004) Structure of the ferrous form of (4-hydroxyphenyl)pyruvate dioxygenase from *Streptomyces avermitilis* in complex with the therapeutic herbicide, NTBC. Biochemistry **43:** 6370–6377

Bruce BD (2001) The paradox of plastid transit peptides: conservation of function despite divergence in primary structure. Biochim Biophys Acta **1541:** 2–21

Cahoon RE, Coughlan SJ, inventors. June 5, 2007. Plant vitamin E biosynthetic enzymes. US Patent No. 7,226,745

Callis J, Carpenter T, Sun CW, Vierstra RD (1995) Structure and evolution of genes encoding polyubiquitin and ubiquitin-like proteins in Arabidopsis thaliana ecotype Columbia. Genetics **139:** 921–939

Crameri A, Raillard SA, Bermudez E, Stemmer WPC (1998) DNA shuffling of a family of genes from diverse species accelerates directed evolution. Nature **391:** 288–291

Dey N, Maiti IB (1999) Structure and promoter/leader deletion analysis of mirabilis mosaic virus (MMV) full-length transcript promoter in transgenic plants. Plant Mol Biol **40:** 771–782

Dixon DP, Edwards R (2006) Enzymes of tyrosine catabolism in *Arabidopsis thaliana*. Plant Sci **171:** 360–366

Duke SO (2012) Why have no new herbicide modes of action appeared in recent years? Pest Manag Sci **68:** 505–512

Emanuelsson O, Nielsen H, Brunak S, von Heijne G (2000) Predicting subcellular localization of proteins based on their N-terminal amino acid sequence. J Mol Biol **300:** 1005–1016

Falco SC, Li Z, inventors. June 22, 2010. S-Adenosyl-L-methionine synthetase promoter and its use in expression of transgenic genes in plants. US Patent No. 7,741,537

Fiedler E, Soll J, Schultz G (1982) The formation of homogentisate in the biosynthesis of tocopherol and plastoquinone in spinach chloroplasts. Planta **155:** 511–515

Fritze IM, Linden L, Freigang J, Auerbach G, Huber R, Steinbacher S (2004) The crystal structures of *Zea mays* and Arabidopsis 4-hydroxyphenylpyruvate dioxygenase. Plant Physiol **134:** 1388–1400

Garcia I, Rodgers M, Lenne C, Rolland A, Sailland A, Matringe M (1997) Subcellular localization and purification of a p-hydroxyphenylpyruvate dioxygenase from cultured carrot cells and characterization of the corresponding cDNA. Biochem J **325:** 761–769

Garcia I, Rodgers M, Pepin R, Hsieh TF, Matringe M (1999) Characterization and subcellular compartmentation of recombinant 4-hydroxyphenylpyruvate dioxygenase from Arabidopsis in transgenic tobacco. Plant Physiol **119:** 1507–1516

Green JM, Castle LA (2010) Transitioning from single to multiple herbicide-resistant crops. *In* VK Nandula, ed, Glyphosate Resistance in Crops and Weeds: History, Development, and Management. Wiley, Hoboken, NJ, pp 67–91

Han C, Ren C, Zhi T, Zhou Z, Liu Y, Chen F, Peng W, Xie D (2013) Disruption of fumarylacetoacetate hydrolase causes spontaneous cell death under short-day conditions in Arabidopsis. Plant Physiol **162:** 1956–1964

Hawkes TR, Langford MP, Viner RC, Vernooij BTM, Dale R, inventors. August 5, 2010. Mutant hydroxyphenylpyruvate dioxygenase polypeptides and methods of use. US Patent Application No. 2010/0197503

Hawkins J, Bodén M (2006) Detecting and sorting targeting peptides with neural networks and support vector machines. J Bioinform Comput Biol **4:** 1–18

Heap I (2014) The International Survey of Herbicide Resistant Weeds. http://www.weedscience.org/summary/MOA.aspx?MOAID=12

Höglund A, Dönnes P, Blum T, Adolph HW, Kohlbacher O (2006) MultiLoc: prediction of protein subcellular localization using N-terminal targeting sequences, sequence motifs and amino acid composition. Bioinformatics **22:** 1158–1165

Horton P, Park KJ, Obayashi T, Fujita N, Harada H, Adams-Collier CJ, Nakai K (2007) WoLF PSORT: protein localization predictor. Nucleic Acids Res **35:** W585–W587

Hu XT, Owens MA (2011) Multiplexed protein quantification in maize leaves by liquid chromatography coupled with tandem mass spectrometry: an alternative tool to immunoassays for target protein analysis in genetically engineered crops. J Agric Food Chem **59:** 3551–3558

Jarvis P (2008) Targeting of nucleus-encoded proteins to chloroplasts in plants. New Phytol **179:** 257–285

Kapila J, De Rycke R, Van Montagu M, Angenon G (1997) An Agrobacterium-mediated transient gene expression system for intact leaves. Plant Sci **122:** 101–108

Klein TM, Wolf ED, Wu R, Sanford JC (1987) High-velocity microprojectiles for delivering nucleic acids into living cells. Nature **327:** 70–73

Lassner M, Wilkinson JQ, inventors. March 18, 2008. Plastid transit peptides. US Patent No. 7,345,143

Lee DW, Lee S, Lee GJ, Lee KH, Kim S, Cheong GW, Hwang I (2006) Functional characterization of sequence motifs in the transit peptide of Arabidopsis small subunit of Rubisco. Plant Physiol **140:** 466–483

Liu Z, Taub CC, McClung CR (1996) Identification of an *Arabidopsis thaliana* ribulose-1,5-bisphosphate carboxylase/oxygenase activase (RCA) minimal promoter regulated by light and the circadian clock. Plant Physiol **112:** 43–51

Löffelhardt W, Kindl H (1979) Conversion of 4-hydroxyphenylpyruvic acid into homogentisic acid at the thylakoid membrane of *Lemna gibba*. FEBS Lett **104:** 332–334

Maeda H, DellaPenna D (2007) Tocopherol functions in photosynthetic organisms. Curr Opin Plant Biol **10:** 260–265

Maeda H, Dudareva N (2012) The shikimate pathway and aromatic amino acid biosynthesis in plants. Annu Rev Plant Biol **63:** 73–105

Matringe M, Sailland A, Pelissier B, Rolland A, Zink O (2005) p-Hydroxyphenylpyruvate dioxygenase inhibitor-resistant plants. Pest Manag Sci **61:** 269–276

Moran GR (2014) 4-Hydroxyphenylpyruvate dioxygenase and hydroxymandelate synthase: exemplars of the α-keto acid dependent oxygenases. Arch Biochem Biophys **544:** 58–68

Moshiri F, Hao M, Karunanandaa B, Valentin HE, Venkatesh TV, Wong YHH, inventors. November 20, 2007. Genes encoding 4-hydroxyphenylpyruvate dioxygenase (HPPD) enzymes for plant metabolic engineering. US Patent No. 7,297,541

Neidig ML, Decker A, Kavana M, Moran GR, Solomon EI (2005) Spectroscopic and computational studies of NTBC bound to the non-heme iron enzyme (4-hydroxyphenyl)pyruvate dioxygenase: active site contributions to drug inhibition. Biochem Biophys Res Commun **338:** 206–214

Ness JE, Kim S, Gottman A, Pak R, Krebber A, Borchert TV, Govindarajan S, Mundorff EC, Minshull J (2002) Synthetic shuffling expands functional protein diversity by allowing amino acids to recombine independently. Nat Biotechnol **20:** 1251–1255

Norris SR, Meyer SE, Callis J (1993) The intron of Arabidopsis thaliana polyubiquitin genes is conserved in location and is a quantitative determinant of chimeric gene expression. Plant Mol Biol **21:** 895–906

Norsworthy JK, Ward SM, Shaw DR, Llewellyn RS, Nichols RL, Webster TM, Bradley KW, Frisvold G, Powles SB, Burgos NR, et al (2012) Reducing the risks of herbicide resistance: best management practices and recommendations. Weed Sci (Suppl 1) **60:** 31–62

Ow DW, Jacobs JD, Howell SH (1987) Functional regions of the cauliflower mosaic virus 35S RNA promoter determined by use of the firefly luciferase gene as a reporter of promoter activity. Proc Natl Acad Sci USA **84:** 4870–4874

Raspail C, Graindorge M, Moreau Y, Crouzy S, Lefèbvre B, Robin AY, Dumas R, Matringe M (2011) 4-Hydroxyphenylpyruvate dioxygenase catalysis: identification of catalytic residues and production of a hydroxylated intermediate shared with a structurally unrelated enzyme. J Biol Chem **286:** 26061–26070

Riewe D, Koohi M, Lisec J, Pfeiffer M, Lippmann R, Schmeichel J, Willmitzer L, Altmann T (2012) A tyrosine aminotransferase involved in tocopherol synthesis in Arabidopsis. Plant J **71:** 850–859

Ruiz-Sola MA, Rodriguez-Conception M (2012) Carotenoid biosynthesis in Arabidopsis: a colorful pathway. The Arabidopsis Book **10:** 1–28, doi/10.1199/tab.0158

Saul H, Elharrar E, Gaash R, Eliaz D, Valenci M, Akua T, Avramov M, Frankel N, Berezin I, Gottlieb D, et al (2009) The upstream open reading frame of the Arabidopsis AtMHX gene has a strong impact on transcript accumulation through the nonsense-mediated mRNA decay pathway. Plant J **60:** 1031–1042

Schein AI, Kissinger JC, Ungar LH (2001) Chloroplast transit peptide prediction: a peek inside the black box. Nucleic Acids Res **29:** E82

Schenck CA, Chen S, Siehl DL, Maeda HA (2014) Non-plastidic, tyrosine-insensitive prephenate dehydrogenases from legumes. Nature Chem Biol, in press.

Schmutz J, Cannon SB, Schlueter J, Ma J, Mitros T, Nelson W, Hyten DL, Song Q, Thelen JJ, Cheng J, et al (2010) Genome sequence of the palaeopolyploid soybean. Nature **463:** 178–183

Secor J (1994) Inhibition of barnyardgrass 4-hydroxyphenylpyruvate dioxygenase by sulcotrione. Plant Physiol **106:** 1429–1433

Shen WJ, Forde BG (1989) Efficient transformation of Agrobacterium spp. by high voltage electroporation. Nucleic Acids Res **17:** 8385

Siehl DL (1999) The biosynthesis of tryptophan, tyrosine, and phenylalanine from chorismate. *In* B Singh, ed, Plant Amino Acids: Biochemistry and Biotechnology. Marcel Dekker, New York, pp 171–204

Siehl DL, Castle LA, Gorton R, Keenan RJ (2007) The molecular basis of glyphosate resistance by an optimized microbial acetyltransferase. J Biol Chem **282:** 11446–11455

Simmons CR, Navarro Acevedo PA, inventors. June 3, 2010. Gene promoter regulatory element analysis computational methods and their use in transgenic applications. US Patent Application No. 20100138952

Smale ST, Kadonaga JT (2003) The RNA polymerase II core promoter. Annu Rev Biochem **72:** 449–479

Sozer O, Komenda J, Ughy B, Domonkos I, Laczkó-Dobos H, Malec P, Gombos Z, Kis M (2010) Involvement of carotenoids in the synthesis and assembly of protein subunits of photosynthetic reaction centers of Synechocystis sp. PCC 6803. Plant Cell Physiol **51:** 823–835

Tzin V, Galili G (2010) New insights into the shikimate and aromatic amino acids biosynthesis pathways in plants. Mol Plant **3:** 956–972

Yang C, Pflugrath JW, Camper DL, Foster ML, Pernich DJ, Walsh TA (2004) Structural basis for herbicidal inhibitor selectivity revealed by comparison of crystal structures of plant and mammalian 4-hydroxyphenylpyruvate dioxygenases. Biochemistry **43:** 10414–10423

Yoo H, Widhalm JR, Qian Y, Maeda H, Cooper BR, Jannasch AS, Gonda I, Lewinsohn E, Rhodes D, Dudareva N (2013) An alternative pathway contributes to phenylalanine biosynthesis in plants via a cytosolic tyrosine:phenylpyruvate aminotransferase. Nat Commun **4:** 2833

Zannoni VG, Lomtevas N, Goldfinger S (1969) Oxidation of homogentisic acid to ochronotic pigment in connective tissue. Biochim Biophys Acta **177:** 94–105

Zhang JH, Dawes G, Stemmer WPC (1997) Directed evolution of a fucosidase from a galactosidase by DNA shuffling and screening. Proc Natl Acad Sci USA **94:** 4504–4509